



A new quantitative index in the diagnosis of Parkinson syndrome by dopamine transporter single-photon emission computed tomography

Ryota Bando¹ · Hideki Otsuka² · Tamaki Otani³ · Noritake Matsuda¹ · Shota Azane¹ · Yamato Kunikane¹ · Yoichi Otomi⁴ · Wataru Sako⁵ · Yuishin Izumi⁵ · Masafumi Harada⁴

Received: 26 July 2020 / Accepted: 28 January 2021 / Published online: 25 February 2021
© The Japanese Society of Nuclear Medicine 2021

Abstract

Objective Dopamine transporter single-photon emission computed tomography (DAT SPECT) has been widely used to diagnose Parkinson syndrome. Using the standardized uptake value (SUV) of DAT SPECT, we propose “functional dopamine transporter volume (f-DTV)” as a new quantitative index to evaluate the three-dimensional volume of functional dopamine transporters and assess its diagnostic ability in differentiating dopaminergic neurodegenerative diseases (dNDD) from non-dNDD.

Methods Seventy-nine patients were enrolled (42 dNDD, 37 non-dNDD; 38 men; age 24–88 years). We analyzed seven quantitative indices. The specific binding ratio (SBR) was calculated using a program specialized for DAT SPECT (SBR_Bolt). The SUV_{max}, SUV_{peak}, and SUV_{mean} were calculated using a quantification program for bone SPECT. SBR_SUV was calculated by dividing striatal SUV_{mean} by the average of background SUV_{mean}. The cutoff value of the active dopamine transporter level was examined using three methods (threshold of 40% of SUV_{max}, SUV 2, and SUV 3) to calculate the active dopamine transporter volume (ADV). The f-DTV was calculated by multiplying ADV and SUV_{mean}. We assessed the correlations between SBR_Bolt and SBR_SUV, and compared the mean value of each index between the dNDD and non-dNDD groups. The abilities of SBR_Bolt, SBR_SUV, SUV_{max}, SUV_{peak}, SUV_{mean}, ADV, and f-DTV in differentiating dNDD from non-dNDD were determined by the area under the receiver operating curve (AUC) generated by the receiver operating characteristics analysis.

Results The SBR_Bolt and SBR_SUV highly correlated with each other ($r=0.71$). The cutoff value of the active dopamine transporter level was determined as SUV 3. All seven quantitative indices showed lower values in the dNDD group than in the non-dNDD group, and the difference between the two groups was statistically significant ($p<0.05$). Sensitivity, specificity, and AUC of f-DTV were slightly lower than those of SBR_Bolt (71%, 79%, and 0.81, respectively, for f-DTV, and 81%, 84%, 0.88, respectively, for SBR_Bolt). The difference in AUC between f-DTV and SBR_Bolt was not statistically significant.

Conclusions This study demonstrates the utility of f-DTV as a novel quantitative index for evaluating the three-dimensional volume of functional dopamine transporters, and that f-DTV has almost the same diagnostic ability to differentiate dNDD from non-dNDD using DAT SPECT.

Keywords Active dopamine transporter volume · Dopamine transporter SPECT · Functional dopamine transporter volume · Parkinson syndrome · SUV

✉ Hideki Otsuka
hideki.otsuka@tokushima-u.ac.jp

¹ Department of Radiology, Tokushima University Hospital, Kuramoto-cho 3-18-15, Tokushima 770-8503, Japan

² Department of Medical Imaging/Nuclear Medicine, Tokushima University Graduate School of Biomedical Sciences, Tokushima, Japan

³ Advance Radiation Research, Education and Management Center, Tokushima University, Tokushima, Japan

⁴ Department of Radiology and Radiation Oncology, Tokushima University Graduate School of Biomedical Sciences, Tokushima, Japan

⁵ Department of Neurology, Tokushima University Graduate School of Biomedical Sciences, Tokushima, Japan

Introduction

Nuclear medicine studies, especially dopamine transporter single-photon emission computed tomography (DAT SPECT) using ^{123}I -ioflupane and ^{123}I -metaiodobenzylguanidine myocardial scintigraphy, play a critical role in the diagnosis of Parkinson syndrome (PS) [1]. DAT SPECT has been widely used to differentiate between PS with presynaptic dopaminergic deficit, such as Parkinson's disease (PD), dementia of Lewy body, multiple stem atrophy, progressive supranuclear palsy, and corticobasal syndrome; and other forms of PS without presynaptic dopaminergic deficit, such as essential tremor, drug-induced parkinsonism, and psychogenic parkinsonism. The dopamine transporter in the striatum decreases in dopaminergic neurodegenerative disease (dNDD) and remains consistent in non-dNDD [2–4]. Image interpretations have been performed using both visual and quantitative analyses, and these two analyses combined can improve the diagnostic accuracy of PS [5–8].

The specific binding ratio (SBR) is the most popular quantitative index used for the evaluation of ^{123}I -ioflupane uptake in the striatum with DAT SPECT [9]. The SBR is defined as the relative ratio of the striatum to the background brain parenchyma. Positron emission tomography (PET) also can be used to perform quantitative analysis. The standardized uptake value (SUV) is one of the most commonly used quantitative indices to demonstrate the degree of PET tracer uptake in a region of interest (ROI). In fluoro-deoxy-glucose (FDG)-PET, the metabolic tumor volume (MTV) and total lesion glycolysis (TLG) are used as additional quantitative indices to evaluate the activity of malignant tumors, as these values can quantify the three-dimensional volume of metabolically active lesions [10]. A program used to calculate the SUV has recently been developed and implemented in bone SPECT using $^{99\text{m}}\text{Tc}$ -hydroxymethylene diphosphonate [11, 12]. Toriihara et al. first introduced the use of SUV in DAT SPECT and reported that the SUV may be a promising marker in the diagnosis of PD [13].

We adapted the SUV for DAT SPECT to develop the novel quantitative indices of active dopamine transporter volume (ADV) and functional dopamine transporter volume (f-DTV) to evaluate the three-dimensional volume of functional dopamine transporters.

Materials and methods

This retrospective study was performed at a single university hospital and received approval from the Tokushima University Hospital ethics committee. Written informed consent was waived. The information disclosure document of this study is available to the public on Tokushima University

Hospital website. Both the phantom and clinical studies were performed using a hybrid SPECT/CT system (Symbia T16; Siemens, Germany).

Phantom study

A phantom experiment was performed to calculate the Bequerel calibration factor (BCF) for converting reformatted SPECT images to the radiation dose. A cylindrical phantom (inner diameter 16 cm, length 15 cm, volume 3016 mL; Sangyo Kagaku, Tokyo, Japan) was prepared with 80 g of sodium dihydrogen citrate, water, and 111 MBq of ^{123}I -IMP. The phantom was scanned for 28 min, and the data were reconstructed according to the clinical DAT SPECT protocol (Table 1). The BCF acquired with bone SPECT analyzing software was used to calculate the SUV in this study (GI-BONE; AZE Corp., Tokyo, Japan).

Patient study

Seventy-nine patients were enrolled in this retrospective study (42 dNDD, 37 non-dNDD; 38 men; age 24–88 years; Table 2). Only in-house patients with confirmed clinical diagnosis by a board-certified neurologist (Y.I.) and with available data on body weight and the injected radiation dose were included; referral patients were excluded. Patients were diagnosed with PD according to the UK Brain Bank criteria [14]. Approximately 167 MBq of ^{123}I -ioflupane was injected intravenously, and the SPECT/CT scan was performed 3 h after injection. CT data were used for attenuation correction and to obtain anatomical information. The triple energy window method was used for scatter correction, and the

Table 1 Image processing

SPECT/CT scanner	Symbia T16 (Siemens)
Collimator	LMEGP
RI	^{123}I
keV	159 keV \pm 10%
Matrix	128 \times 128
Pixel size	3.3 mm
Image processing	Continuous mode
Rotation	180°
Collection time	3.5 min \times 8
Attenuation correction	CTAC
Scatter correction	TEW
Filter	
OSEM	Gaussian 6.6 mm
OSEM	
Subset number	6
Iterations	12

Table 2 Patient characteristics

	dNDD	Non-dNDD	<i>p</i> value
Number of patients	42	37	–
Men/women	23/19	15/22	0.206
Age: mean (range)	71.8 (42–86)	68.3 (24–88)	0.106
Body weight: mean (SD)	56.8 (12.0)	56.2 (12.6)	0.531
	PD 25	Essential tremor 13	
	DLB 7	Vascular Parkinsonism 4	
	PSP 5	Drug-induced Parkinsonism 3	
	CBS 4	Psychogenic 2	
	MSA 1	iNPH 2	
		Dementia 2	
		Others 11	
		Chorea, dystonia, myopathy, cervical myelopathy, depression, facial spasm, epilepsy, ALS, bipolar disorder, ADCY5, SCD	

dNDD dopaminergic neurodegenerative disease, *PD* Parkinson disease, *DLB* dementia of Lewy body, *MSA* multiple stem atrophy, *PSP* progressive supranuclear palsy, *CBS* corticobasal syndrome, *SCD* spinocerebellar degeneration, *MSA* multiple system atrophy, *PSP* progressive supranuclear palsy, *iNPH* idiopathic normal pressure hydrocephalus, *ALS* amyotrophic lateral sclerosis, *FTD with depression* frontotemporal dementia with depression

resulting image was reconstructed using the ordered-subset expectation maximization (OSEM) method.

Quantitative indices

We calculated all indices in both the right and left striatum separately, and the lower values were included in the analysis.

SBR_Bolt

The SBRs were calculated using DaTView (AZE Corp., Tokyo, Japan), a software specialized for DAT SPECT and based on Bolt's method. A slab thickness of approximately 44 mm was automatically set centered on the striatum (Fig. 1a) [4, 9]. We named the SBR calculated by DaTView as SBR_Bolt to distinguish it from the SBRs used in other methods. The SBR_Bolt was calculated with the following formula:

$$\text{SBR_Bolt} = C_s/C_n_s,$$

where C_s and C_n_s indicate the specific concentration in the striatum (s) and the nonspecific concentration in the cortex as the reference (r), respectively. They were calculated using the following formulae: $C_s = [(total\ count\ of\ sVOI) - C_n_s \times (total\ volume\ of\ sVOI)]/V_s$, $C_n_s = [(total\ count\ of\ rVOI)/(total\ volume\ of\ rVOI)]$, where $V_s = 11.2$ mL. Nonspecific reference concentration was defined as the average count of the brain parenchyma, except the striatum.

SUV

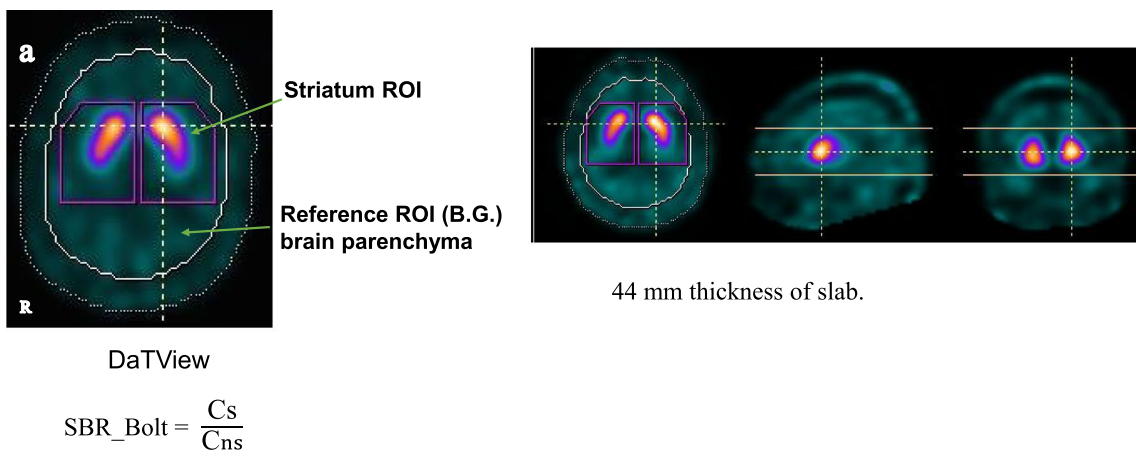
The radiation count was converted to radioactivity using the BCF as follows: radioactivity of the region (Bq) = (radiation count of the region) × BCF. Using the quantification software program for bone SPECT (GI-BONE; AZE Corp., Tokyo, Japan; Fig. 1b), SUV was calculated using the following formula: $SUV = \text{mean } ROI \text{ activity (MBq/g)} / [\text{injected dose (MBq)} / \text{body weight (g)}] = [(\text{total count of } ROI) \times \text{BCF} / \text{the volume of } ROI] / [\text{injected dose} / \text{body weight}]$. The SUV of each striatum was measured separately by using the previous BCF. To set an ROI, 40% of the SUVmax of the striatum of the patient, which is the default value of GI-BONE, was used as the threshold. The SUVmax, SUVpeak, and SUVmean were calculated. To compare with SBR_Bolt, SBR_SUV by GI-BONE was calculated using the following formula:

$SBR_SUV = \text{lower value of striatal SUVmean} / \text{average of BG SUVmean}$ (BG, background; occipital parenchyma as BG) [13].

We proposed the following two new quantitative indices for DAT SPECT: f-DTV and ADV.

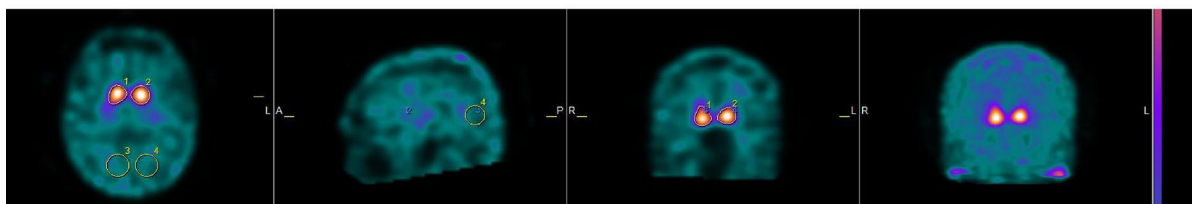
Active dopamine transporter volume

The ADV indicates the active dopamine transporter volume and corresponds to the MTV on FDG-PET. It represents the volume of voxels with an SUV exceeding the cutoff value. The region exceeding the cutoff value was considered functionally active. The cutoff value was examined using the following three methods (Fig. 2): (1) a threshold of 40% of



$Cns = [(total\ count\ of\ rVOI) / (total\ volume\ of\ rVOI)]$
 $Cs = [(total\ count\ of\ sVOI) - Cns \times (total\ volume\ of\ sVOI)] / Vs$
 $Vs = 11.2ml$

a



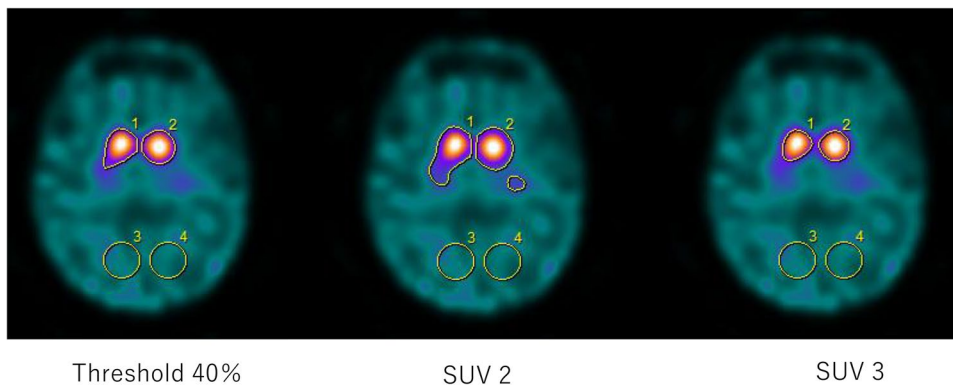
$SBR_SUV = sSUVmean / average\ of\ BGSUVmean$
 s: striatum, BG: background, occipital parenchyma as a reference

b

Fig. 1 a VOI setting on DaTView. $SBR = Cs/Cns$. $Cs = [(total\ count\ of\ sVOI) - Cns \times (total\ volume\ of\ sVOI)] / Vs$, $Cns = [(total\ count\ of\ rVOI) / (total\ volume\ of\ rVOI)]$. $Vs = 11.2\ ml$. Cs ; the specific concentration in the striatum. Cns ; the nonspecific concentration in brain

cortex. **b** VOI setting on GI-BONE. $SBR_SUV = sSUVmean / average\ of\ BGSUVmean$. s: striatum, BG background, occipital parenchyma as a reference

Fig. 2 VOI setting on GI-BONE for ADV



SUVmax of the lower side of striatum, (2) SUV 2, and (3) SUV 3.

The diagnostic abilities of each method in differentiating dNDD from non-dNDD were assessed using receiver operating characteristic (ROC) analysis and the area under the curve (AUC). The difference of AUC was examined using the Chi-square test.

Functional dopamine transporter volume

The cutoff value that had the highest AUC for ADV was adapted to calculate the f-DTV.

The f-DTV reflects the total functional dopamine transporter volume and corresponds to the TLG value on FDG-PET. We calculated the f-DTV using the following formula:

$$\text{f-DTV} = \text{ADV} \times \text{SUVmean.}$$

The diagnostic abilities of the SBR_Bolt, SBR_SUV, SUVmax, SUVpeak, SUVmean, ADV, and f-DTV in differentiating dNDD from non-dNDD were also assessed using ROC analysis and the AUC.

Statistical analyses

A Chi-square test and Student's *t* test were used to compare patient characteristics such as sex, age, and body weight. Student's *t* test was used to compare each index (SBR_Bolt, SBR-SUV, SUVmax, SUVpeak, SUVmean, ADV, and f-DTV) between the dNDD and non-dNDD groups. A *p* value of <0.05 was considered to indicate statistical significance.

To clarify the relationship between the SBR_Bolt and SBR_SUV, the correlation coefficient (*r* value) was calculated. ROC curve analysis was used to set the cutoff value and evaluate the sensitivity, specificity, test accuracy, and AUC of each quantitative index. The difference of AUC was examined using the Chi-square test.

Results

The seven quantitative indices are shown in Table 3. All index values were lower in the dNDD group than those in the non-dNDD group, and the difference between the two groups was statistically significant. The correlation between SBR_SUV and SBR_Bolt is shown in Fig. 3. The SBR_SUV highly correlated with SBR_Bolt ($r=0.71$). The statistical results of the ROC analysis of the cutoff value for ADV are shown in Fig. 4. Method 3 (SUV 3) was statistically superior to the other two methods and had the highest AUC value (0.79). Tables 4, 5, and Fig. 5 show the ROC results of the cutoff value and the diagnostic ability of differentiating dNDD from non-dNDD. The sensitivity, specificity, and accuracy of f-DTV were slightly inferior to those of SBR_Bolt. AUC showed almost the same value in f-DTV (0.81) and SBR_Bolt (0.88). The difference of AUC between f-DTV and SBR_Bolt was not statistically significant. Figure 6 shows the dNDD and non-dNDD patient images and each index. The uptake of ^{123}I -ioflupane in the bilateral striatum was markedly decreased, showing a dot-like appearance in a patient with PD (Fig. 6a, b). The uptake was preserved in a patient without PD (Fig. 6c, d). The patient was diagnosed with essential tremor.

Discussion

Parkinsonism symptoms such as tremor, rigidity, and bradykinesia present in diseases both with and without presynaptic dopaminergic deficit. DAT SPECT can image the dopamine transporter function, and assist the differential diagnosis of PS. Visual and quantitative analyses are performed (and usually combined) to assess the DAT SPECT [4, 7, 8].

A visual assessment of the DAT scan was performed to evaluate the shape and degree of the ioflupane uptake in the striatum. The classification of striatal uptake pattern and degree is useful in the diagnosis of uncertain Parkinsonian syndrome and in the differential diagnosis between PD and atypical Parkinsonian syndromes [15, 16]. The striatal uptake of ioflupane was uniform in the healthy brain and appeared as symmetrical, comma-shaped patterns in the left and right hemispheres. Conversely, the uptake in patients with presynaptic dopaminergic deficit was diminished. The striatal uptake pattern differs between PD and atypical Parkinsonian syndromes, and in the subtypes of early PD. PD first appears as reduced accumulation in the putamen (eagle wing), whereas more severe cases often exhibit egg-shaped patterns, lower total uptake, and left–right asymmetry (mixed type). Visual assessments are influenced by the set “window level”, which requires a standardized view.

Table 3 Quantitative index

	dNDD	Non-dNDD	<i>p</i> value
SBR_Bolt	3.52 (1.71)	6.49 (2.0)	<0.05
SBR_SUV	2.25 (0.47)	3.00 (0.74)	<0.05
SUVmax	7.2 (2.3)	9.7 (1.7)	<0.05
SUVpeak	6.1 (1.9)	8.3 (1.3)	<0.05
SUVmean	3.0 (0.4)	3.6 (0.3)	<0.05
ADV	27.1 (14.1)	32.3 (9.1)	<0.05
f-DTV	85.8 (47.0)	120.4 (35.9)	<0.05
		Mean (SD)	

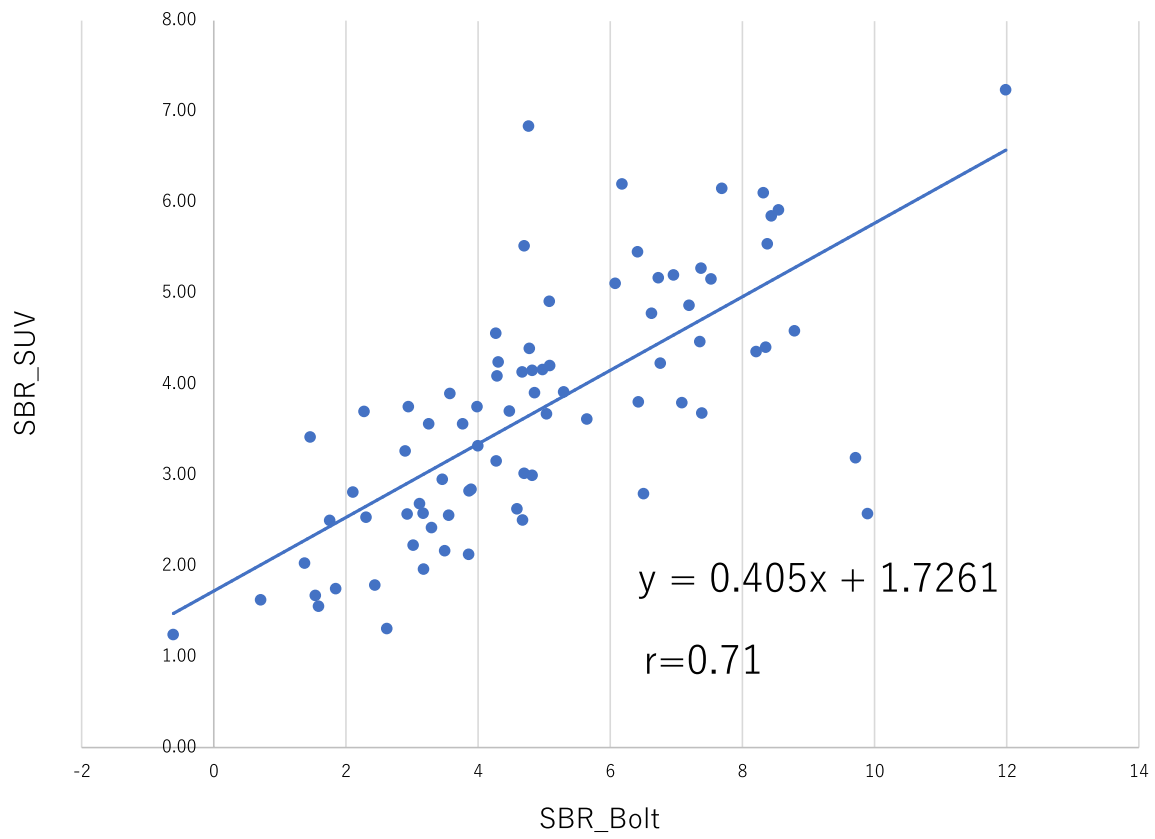
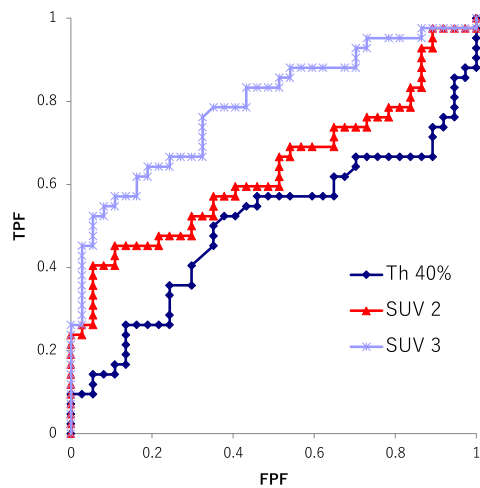


Fig. 3 The correlation between SBR_Bolt and SBR_SUV

Fig. 4 ROC analysis of cutoff value for ADV



cutoff	AUC
Th 40%	0.50
SUV 2	0.64
SUV 3	0.79

Cutoff 1	Cutoff 2	<i>p</i> value, chi-square test
Th 40%	SUV 2	0.0975
Th 40%	SUV 3	<i>p</i> < 0.05
SUV 2	SUV 3	<i>p</i> < 0.05

Table 4 ROC analysis (value)

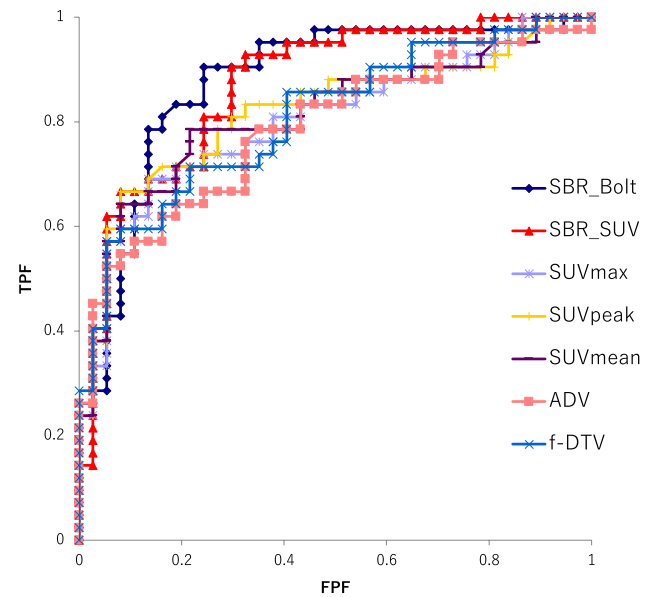
	Cutoff	Sensitivity (%)	Specificity (%)	Accuracy (%)	AUC
SBR_Bolt	4.68	81	84	82	0.88
SBR_SUV	3.75	81	76	80	0.87
SUVmax	8.1	69	86	77	0.80
SUVpeak	7.2	71	84	77	0.82
SUVmean	4.9	79	78	78	0.81
ADV	15.2	76	68	72	0.79
f-DTV	65.1	71	78	75	0.81

Table 5 Statistical analysis

Index 1	Index 2	<i>p</i> value, Chi-square test
SBR_Bolt	SBR_SUV	0.8707
SBR_Bolt	SUVmax	0.1586
SBR_Bolt	SUVpeak	0.2464
SBR_Bolt	SUVmean	0.2070
SBR_Bolt	ADV	0.0571
SBR_Bolt	f-DTV	0.1275
SBR_SUV	SUVmax	0.1268
SBR_SUV	SUVpeak	0.2537
SBR_SUV	SUVmean	0.1839
SBR_SUV	ADV	0.1276
SBR_SUV	f-DTV	0.2223
SUVmax	SUVpeak	0.2255
SUVmax	SUVmean	0.3782
SUVmax	ADV	0.6548
SUVmax	f-DTV	0.8635
SUVpeak	SUVmean	0.6077
SUVpeak	ADV	0.3259
SUVpeak	f-DTV	0.7247
SUVmean	ADV	0.4634
SUVmean	f-DTV	0.8800
ADV	f-DTV	*0.0364 < 0.05

*Statistically significant

In regular clinical practice, conventional SPECT images and normalized images are usually assessed in parallel with DaTView to inform diagnoses. In addition to visual analysis, quantitative indices are essential for rendering a differential diagnosis of PS, evaluating disease severity, and assessing patients during follow-up. SBR and asymmetry index (AI) are two established quantitative indices used to evaluate changes over time in clinical severity and striatal degeneration in PD. Tossici-Bolt et al. proposed SBR as a quantitative index that could measure the specific binding of the tracer in the striatum [9]. In the present study, SBR_Bolt was calculated by DaTView based on the Bolt's method, in which a slab with a thickness of 44 mm was set to reduce

**Fig. 5** ROC curve analysis for quantitative index

the partial volume effect. SBR is affected by some technical and methodological variances. Some studies have reported that using a modified version of Bolt's method, new indices, and software other than DaTView improves the accuracy of diagnosing PS [17, 18]. SBR varies according to the gamma camera system, image reconstruction methods [ordered-subset expectation maximization (OSEM) or filtered backprojection (FBP)], with/without attenuation (CT attenuation correction or Chang correction), and scatter correction [19–21]. Bienkiewicz et al. reported that OSEM reconstruction with CT attenuation correction can achieve better intra-operator reproducibility relative to FBP reconstruction with Chang attenuation correction [17]. Rahman et al. reported the utility of a new count-based method to extract the striatal volume for SBR calculations [22]. Bolt et al. also reported a DAT normal database and showed that the normal range of SBR is widely distributed and decreases with aging [20]. Several studies have already assessed the utility of SBR in diagnostics; however, the mean SBR of both dNDD and non-dNDD groups, which is the cutoff SBR value for differential diagnosis and diagnostic ability, differ among reports. Compared to that in the report by Toriihara et al. the SBR generated in this study (SBR_Bolt) was inferior in accuracy, sensitivity, and specificity, whereas the cutoff value in our study was larger [13]. We speculated that this discrepancy with the previously published study may be attributable to differences in imaging equipment, image reconstruction methods, and patient characteristics such as age distribution, variety of diseases in the non-dNDD group, the severity of dopaminergic degeneration, and the SBR calculation method (Bolt's method or others). We reconstructed the data using OSEM and applied CT attenuation correction,

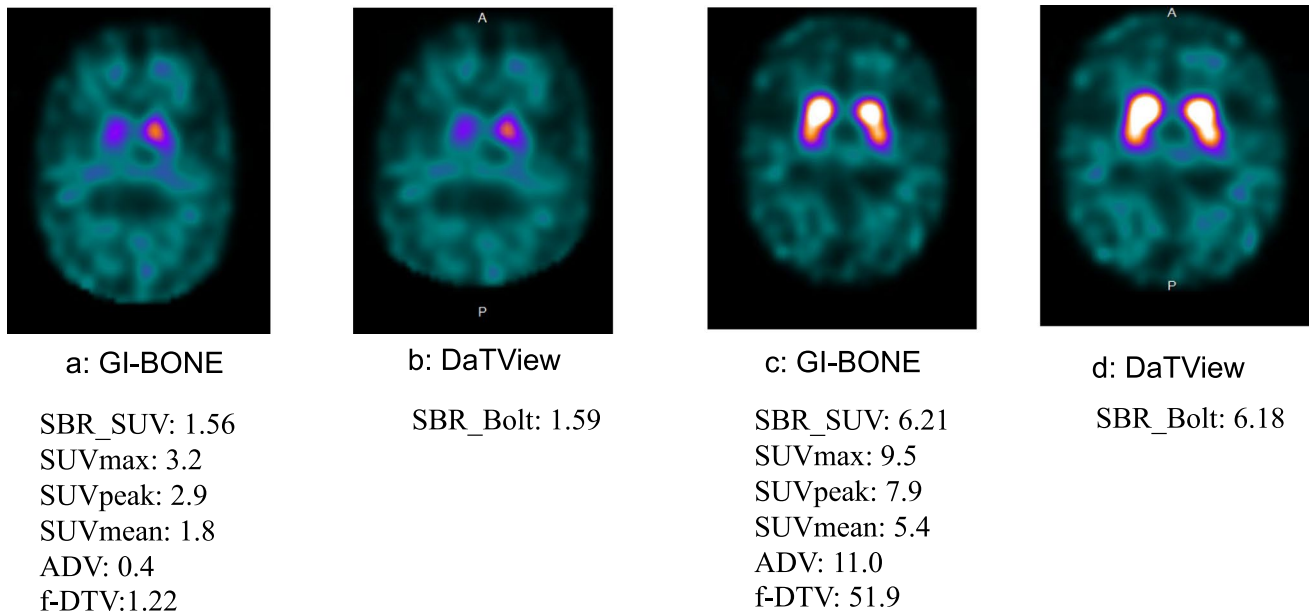


Fig. 6 Images of PD (**a**, **b**) and non-dNDD (essential tremor) (**c**, **d**) and its index. **a** GI-BONE. SBR_SUV: 1.56, SUVmax: 3.2, SUVpeak: 2.9, SUVmean: 1.8, ADV: 0.4, f-DTV:1.22. **b** DaTView.

SBR; 1.59. **c** GI-BONE. SBR_SUV: 6.21, SUVmax: 9.5, SUVpeak: 7.9, SUVmean: 5.4, ADV: 11.0, f-DTV: 51.9. **d** DaTView. SBR; 6.18

and scatter correction. This means that every imaging center needs to independently configure the range for SBR in both affected and unaffected patients; in the case of multicenter studies, scanners should be calibrated to the same settings.

SBR_Bolt is not directly equivalent to the tracer uptake in an absolute sense; instead, it is the relative ratio of the striatal to the brain uptake. Iwabuchi et al. proposed the fractal dimension as a new quantitative indicator and showed that the combined use of SBR and fractal dimension can improve the accuracy of diagnosing PS (AUC 0.964), and reported the impact of the machine-learning technique [23, 24]. The SUV, another widely used quantitative index in PET imaging, is also a relative measure that represents the local uptake corrected by the tracer dose and body weight. The BCF must be calculated specifically for the scanner to correctly estimate the SUV. Some studies have been performed on the diagnostic ability of SBR and SUV [13, 24, 25]. Toriihara et al. used the lower SUV of the right or left striatum of each index, such as SUVmax, SUVpeak, SUVmean, and SUVratio (striatal SUVmean/occipital SUVmean), to inform the differential diagnosis of PD and concluded that its classification performance was slightly inferior to that of SBR [13]. The SBR_SUV in the present study corresponded to the SUVratio reported by Toriihara et al. The SBR_SUV and SBR_Bolt highly correlated with each other ($r=0.71$). The difference between SBR_Bolt and SBR_SUV is the presence or absence of background subtraction; SBR_Bolt applies the background subtraction. Compared to SBR_Bolt, the sensitivity, specificity, and accuracy were slightly lower to almost

equal, and the AUC was slightly lower in SBR_SUV, SUVmax, SUVpeak, and SUVmean compared to SBR_Bolt, but the difference was not statistically significant. In this study, we applied the SUV, the quantitative index most common in PET studies for the DAT SPECT analysis, to propose a new index: f-DTV, which corresponds to TLG in PET and defined the ADV as MTV in PET using GI-BONE. We considered the region exceeding the threshold value as a functionally active dopamine transporter. To calculate the ADV, the optimal threshold of the SUV is necessary. With this analysis software, a VOI is drawn automatically after inputting the cutoff value of the SUV. We applied three methods for the SUV setting. Method 1 is the default value of GI-BONE, set at 40% of the threshold of the SUVmax in the striatum of each patient. However, this method presents some difficulties, as the SUVmax can vary for each patient, resulting in a possible change in the level of the active transporter in each patient. Method 2 uses the SUV 2. The mean SUVmax of background (occipital brain parenchyma) was 2.1 in the dNDD group and 1.9 in the non-dNDD group, and the difference between the two groups did not show statistical significance with the t test. We considered an exceeding uptake over background as functionally active, and we set SUV 2 as the cutoff value. We examined SUV 3 that is 1 greater than 2 in method 3. Anatomical striatal VOI and functional VOI were mismatched (Fig. 2). In the three methods, SUV 3 showed the largest AUC, and the difference between the others was statistically significant ($p < 0.05$, chi-square test). This method most adequately draws the VOI.

We set the SUV threshold to 3 to calculate the ADV and f-DTV. Regions with an SUV > 3 were considered active and to feature functional dopamine transporters.

The f-DTV, which is equal to the product of the ADV and SUVmean, allowed us to explore the spatial distribution of dopamine transporter functionality in three dimensions and consider its diagnostic power of differentiating the dopaminergic deficit disease in Parkinsonism. Achieving a sensitivity of 71%, specificity of 78%, accuracy of 75%, and AUC of 0.81, the f-DTV was slightly inferior with almost the same diagnostic ability compared to conventional SBR. Every institution can assess this method with reference to the original BCF of the gamma camera and with the introduction of analysis software.

This study had some limitations. First, as this study was performed at a single university hospital, our patient population was limited. The data regarding patient body weight and injection radiation dose are necessary to calculate the quantitative index with GI-BONE. Every injection dose has been recorded in the hospital's information system, and the patients with no body weight data were excluded from the study. This contributed to the lower number of patients. A multicenter study with a larger population is necessary to confirm the utility of the new index f-DTV with GI-BONE in reference to the original BCF of each institution. Calibration of the gamma camera systems is also necessary to normalize and standardize the method. Second, the most adequate SUV threshold of ADV is controversial. We defined the accumulated region of SUV > 3 as a functional dopamine transporter; f-DTV was zero in patients with severe deficit of the transporter with an SUVmax of less than 3. Hence, evaluating patients with severe decreased uptake remains challenging. Third, there was a discrepancy in the VOI settings. The morphological VOI and functional VOI mismatched in patients with dNDD. Some VOIs of the striatum were drawn smaller than its anatomical volume. GI-BONE was developed for bone SPECT, and can calculate the functional volume. DaTView has established a method for VOI setting. Technical improvement may be necessary in VOI settings of the striatum for DAT SPECT. A new software with GI-BONE and DaTView combined function is expected.

Conclusion

The present study adapted the SUV, a quantitative index conventionally used in PET, for use in DAT SPECT. The SBR_SUV and SBR_Bolt were highly correlated. In addition, we proposed f-DTV as a new quantitative index that has almost the same ability as SBR regarding the differential diagnosis of dNDD from non-dNDD. Our method achieved an accuracy of 75% and an AUC of 0.81 when the VOI was set to a cutoff of SUV > 3. The f-DTV may provide a new

reliable quantitative index alongside the conventionally used SBR for the diagnosis of Parkinsonism.

References

1. Uyama N, Otsuka H, Shinya T, Otomi Y, Harada M, Sako W, et al. The utility of the combination of a SPECT study with [123I]-FP-CIT of dopamine transporters and [123I]-MIBG myocardial scintigraphy in differentiating Parkinson disease from other degenerative parkinsonian syndromes. *Nucl Med Commun.* 2017;38:487–92. <https://doi.org/10.1097/MNM.0000000000000674>.
2. Kägi G, Bhatia KP, Tolosa E. The role of DAT-SPECT in movement disorders. *J Neurol Neurosurg Psychiatry.* 2010;81(1):5–12. <https://doi.org/10.1136/jnnp.2008.157370>.
3. Varrone A, Halldin C. Molecular imaging of the dopamine transporter. *J Nucl Med.* 2010;51(9):1331–4. <https://doi.org/10.2967/jnumed.109.065656>.
4. JSNM (Japanese Society of Nuclear Medicine). Clinical practice guideline for dopamine transporter imaging with ¹²³I-ioflupane SPECT ver.2 JSNM 2017
5. Ueda J, Yoshimura H, Shimizu K, Hino M, Kohara N. Combined visual and semi-quantitative assessment of (123)I-FP-CIT SPECT for the diagnosis of dopaminergic neurodegenerative diseases. *Neurol Sci.* 2017;38:1187–91. <https://doi.org/10.1007/s10072-017-2936-3>.
6. Davidsson A, Georgiopoulos C, Dizdar N, Granerus G, Zachrisson H. Comparison between visual assessment of dopaminergic degeneration pattern and semi-quantitative ratio calculations in patients with Parkinson's disease and atypical Parkinsonian syndromes using DaTSCAN® SPECT. *Ann Nucl Med.* 2014;28:851–9. <https://doi.org/10.1007/s12149-014-0878-x>.
7. Nicastro N, Garibotto V, Allali G, Assal F, Burkhard PR. Added value of combined semi-quantitative and visual [123I]FP-CIT SPECT analyses for the diagnosis of dementia with Lewy bodies. *Clin Nucl Med.* 2017;42:e96–102. <https://doi.org/10.1097/RLU.0000000000001477>.
8. Mäkinen E, Joutsa J, Johansson J, Mäki M, Seppänen M, Kaasinen V. Visual versus automated analysis of [I-123]FP-CIT SPECT scans in parkinsonism. *J Neural Transm.* 2016;123:1309–18. <https://doi.org/10.1007/s00702-016-1586-6>.
9. Tossici-Bolt L, Hoffmann S, Kemp P, Mehta R, Fleming J. Quantification of [123I]FP-CIT SPECT brain images: an accurate technique for measurement of the specific binding ratio. *Eur J Nucl Med Mol Imaging.* 2006;33:1491–9. <https://doi.org/10.1007/s00259-006-0155-x>.
10. Kaira K, Higuchi T, Naruse I. Metabolic activity by (18)F-FDG-PET/CT is predictive of early response after nivolumab in previously treated NSCLC. *Eur J Nucl Med Mol Imaging.* 2018;45:56–66. <https://doi.org/10.1007/s00259-017-3806-1>.
11. Wei H, Weihao Z, Jiadong X, Hacker M, Bertling J, Lewis R, et al. Standardized uptake values of ^{99m}Tc-MDP SPECT bone scans - a novel method for absolute SPECT/CT quantification. *J Nucl Med* 2015;56(Suppl 3):1790
12. Kuji I, Yamane T, Seto A, Yasumizu Y, Shirotake S, Oyama M. Skeletal standardized uptake values obtained by quantitative SPECT/CT as an osteoblastic biomarker for the discrimination of active bone metastasis in prostate cancer. *Eur J Hybrid Imaging.* 2017;1:2. <https://doi.org/10.1186/s41824-017-0006-y>.
13. Toriihara A, Daisaki H, Yamaguchi A, Kobayashi M, Furukawa S, Yoshida K, et al. Semiquantitative analysis using standardized uptake value in ¹²³I-FP-CIT SPECT/CT. *Clin Imaging.* 2018;52:57–61. <https://doi.org/10.1016/j.clinimag.2018.06.009>.

14. Hughes AJ, Daniel SE, Kilford L, Lees AJ. Accuracy of clinical diagnosis of idiopathic Parkinson's disease: a clinico-pathological study of 100 cases. *J Neurol Neurosurg Psychiatry*. 1992;55:181–4. <https://doi.org/10.1136/jnnp.55.3.181>.
15. Catafau AM, Tolosa E. Impact of dopamine transporter SPECT using ¹²³I-Ioflupane on diagnosis and management of patients with clinically uncertain Parkinsonian syndromes. *Mov Disord*. 2004;19:1175–82. <https://doi.org/10.1002/mds.20112>.
16. Spiegel J, Hellwig D, Samnick S, Jost W, Möllers MO, Fassbender K, et al. Striatal FP-CIT uptake differs in the subtypes of early Parkinson's disease. *J Neural Transm*. 2007;114:331–5. <https://doi.org/10.1007/s00702-006-0518-2>.
17. Bienkiewicz M, Górska-Chrzastek M, Siennicki J, Gajos A, Bogucki A, Mochecka-Thoelke A, et al. Impact of CT based attenuation correction on quantitative assessment of DaTSCAN ((123)I-Ioflupane) imaging in diagnosis of extrapyramidal diseases. *Nucl Med Rev Cent East Eur*. 2008;11:53–8.
18. Miyai M, Yamamoto Y, Uchibe T, Yada N, Haramoto M, Katsube T, et al. Comparison of quantitative value of dopamine transporter scintigraphy calculated from different analytical software. *Nihon Hoshasen Gijutsu Gakkai Zasshi*. 2015;71:1209–14. https://doi.org/10.6009/fjrt.2015_JSRT_71.12.1209 ([Article in Japanese]).
19. Tossici-Bolt L, Dickson JC, Sera T, Nijs R, Bagnara MC, Jonsson C, et al. Calibration of gamma camera systems for a multicentre European ¹²³I-FP-CIT SPECT normal database. *Eur J Nucl Med Mol Imaging*. 2011;38:1529–40. <https://doi.org/10.1007/s00259-011-1801-5> (Epub 2011 Apr 6).
20. Tossici-Bolt L, Dickson JC, Sera T, Booi J, Asenbaun-Nan S, Bagnara MC, Borghat TV, et al. [¹²³I]FP-CIT ENC-DAT normal database: the impact of the reconstruction and quantification methods. *EJNMMI Phys*. 2017;4:8. <https://doi.org/10.1186/s40658-017-0175-6> (Epub 2017 Jan 28).
21. Kameiyama H, Matsutomo N, Nagaki A, Fusae YF. Effect of reconstruction strategies for the quantification and diagnostic accuracy of (123)I-FP-CIT SPECT. *Nihon Hoshasen Gijutsu Gakkai Zasshi*. 2016;72:595–601. https://doi.org/10.6009/fjrt.2016_JSRT_72.7.595 (Article in Japanese).
22. Rahman MGM, Islam MM, Tsujikawa T, Kiyono Y, Okazawa H. Count-based method for specific binding ratio calculation in [I-123]FP-CIT SPECT analysis. *Ann Nucl Med*. 2019;33:14–21. <https://doi.org/10.1007/s12149-018-1297-1> (Epub 2018 Oct 1).
23. Iwabuchi Y, Nakahara T, Kameyama M, Yamada Y, Hashimoto M, Ogata Y, et al. Quantitative evaluation of the tracer distribution in dopamine transporter SPECT for objective interpretation. *Ann Nucl Med*. 2018;32:363–71. <https://doi.org/10.1007/s12149-018-1256-x> (Epub 2018 Apr 13).
24. Iwabuchi Y, Nakahara T, Kameyama M, Yamada Y, Hashimoto M, Matsusaka Y, et al. Impact of a combination of quantitative indices representing uptake intensity, shape, and asymmetry in DAT SPECT using machine learning: comparison of different volume of interest settings. *EJNMMI Res*. 2019;9:7. <https://doi.org/10.1186/s13550-019-0477-x>.
25. Wakabayashi Y, Takahashi R, Kanda T, Zeng F, Nogami M, Ishii K, et al. Semi-quantitative dopamine transporter standardized uptake value in comparison with conventional specific binding ratio in ¹²³I-FP-CIT single-photon emission computed tomography (DaTscan). *Neurol Sci*. 2018;39:1401–7. <https://doi.org/10.1007/s10072-018-3437-8>.

Publisher's Note Springer Nature remains neutral with regard to jurisdictional claims in published maps and institutional affiliations.